DOI: 10.3901/CJME.2016.1021.124, available online at www.springerlink.com; www.cjmenet.com

Data Driven CAN Node Reliability Assessment for Manufacturing System

ZHANG Leiming[1], YUAN Yong[1], and LEI Yong[1, 2, *]

1 *State Key Laboratory of Fluid Power & Mechatronic Systems, Zhejiang University, Hangzhou 310027, China*
2 *State Key Laboratory of Automotive Safety and Energy, Tsinghua University, Beijing 100084, China*

Received April 28, 2016; revised September 27, 2016; accepted October 21, 2016

Abstract: The reliability of the Controller Area Network(CAN) is critical to the performance and safety of the system. However, direct bus-off time assessment tools are lacking in practice due to inaccessibility of the node information and the complexity of the node interactions upon errors. In order to measure the mean time to bus-off(MTTB) of all the nodes, a novel data driven node bus-off time assessment method for CAN network is proposed by directly using network error information. First, the corresponding network error event sequence for each node is constructed using multiple-layer network error information. Then, the generalized zero inflated Poisson process(GZIP) model is established for each node based on the error event sequence. Finally, the stochastic model is constructed to predict the MTTB of the node. The accelerated case studies with different error injection rates are conducted on a laboratory network to demonstrate the proposed method, where the network errors are generated by a computer controlled error injection system. Experiment results show that the MTTB of nodes predicted by the proposed method agree well with observations in the case studies. The proposed data driven node time to bus-off assessment method for CAN networks can successfully predict the MTTB of nodes by directly using network error event data.

Keywords: bus-off, monitoring, Controller Area Network, industrial automation

1 Introduction

Controller Area Network(CAN) based industrial networks, especially DeviceNet and CANopen networks, are widely used in manufacturing applications due to mature hardware and software development supports, ease of configuration and installation, and low maintenance costs. In these systems, a reliable network is essential for continuous production and quality assurance due to the role of the network as the carrier of information and the costs associated with the system downtimes. However, as the networked systems underwent continuous operation with maintenance and reconfigurations in harsh environments, the health condition of the network will deteriorate and affect the performance of the network. Hence, network health monitoring is crucial for system health management and maintenance operations.

In automotive manufacturing systems, node reliability degradation may cause part quality or even safety problems[1–2]. According to CAN specification, each node is embedded with a transmit error counter(TEC). A node will turn to bus-off state if its TEC value exceeds 255 to prevent further disturbances to the network. However, missing a node in these systems will halt the production, and the affected network segment needs human intervention to recovery. Although node state monitoring is of great importance, there is a lack of systematic node reliability assessment method. Therefore, CAN node health assessment tools are highly demanded for monitoring and continuous improvement of the system maintenance.

In literature, some studies has been conducted on reliability assessment for CAN networks. For example, GAUJAL, et al[3], studied the behavior of a node's TEC value using a discrete time Markov chain, whose probability transfer matrix was obtained indirectly from bit error rate(BER). Similar work can be seen in Ref. [4]. LEI, et al[5], studied the bus-off time prediction of the CAN node based on the error distribution within the PLC polling cycles for intermittent connection problems. CAUFFRIEZ, et al[6] and JUMEL, et al[7], studied the network dependability of the distributed systems, especially at the controller level. CORNO, et al[8], studied the dependability of the CAN based networked systems using simulation models. Moreover, the performance analysis of CAN networks under different fault conditions had been studied. HANSSON, et al[9], studied the schedulability of CAN network under fault as a reliability measure. GUJARATI, et al[10], developed a probabilistic analysis that quantified the

* Corresponding author. E-mail: ylei@zju.edu.cn
Supported by National Natural Science Foundation of China(Grant No. 51475422), Science Fund for Creative Research Groups of National Natural Science Foundation of China(Grant No. 51521064), National Basic Research Program of China(973 Program, Grant No. 2013CB-035405), and Open Foundation of State Key Laboratory of Automotive Safety and Energy, Tsinghua University, China(Grant No. KF13011)

tradeoff between fault tolerant and timeliness in CAN network. TRAN, et al[11], studied the multiple-bit error vulnerabilities in different BER environments in a CAN network. RODRIGUEZ-NAVAS, et al[12], discussed the effects of the errors on the packets transmission by constructing an error insertion system for CAN network. Similar concept is also developed in Ref. [13]. SHORT, et al[14], developed a Markov model-based algorithm for data scheduling while guaranteeing the reliability of message delivery in the presence of burst errors in TDMA-based CAN networks. CHEN, et al[15], developed a robust error detection and fault confinement mechanism for CAN network. CENA, et al[16], developed a software based testing system that can inject different types of CAN errors, which is useful for assessment of the synchronization and error handling of a CAN controller. In addition, new system architectures were developed to improve the CAN network reliability. BARRANCO, et al[17], proposed the design of CAN networked structure and solved dependability limitations by means of the active hub. YARAMASU, et al[18], used the impedance function to describe behavior transformation caused by intermittent connection fault on aircraft cable system. BARRANCO, et al[19–20], studied the reliability issues of the CANcentrate bus system. Furthermore, PRODANOV, et al[21], developed a simulation tool to study the impacts of network faults by constructing node behavior models. LEI, et al[22–24], developed a model based monitoring method for intermittent connection problems on CAN networks, and proposed a method to detect and locate the position of the intermittent connection problem.

As shown, the mean time to bus-off state(MTTB) is a direct quantitative measure of the node reliability. However, two challenges need to be tackled to assess the node MTTB of the CAN network: (1) The error counters embedded in the node hardware, which are directly related to the MTTB of the node, are generally inaccessible; (2) According to the CAN specification, the error packet in the CAN network only contains six consecutive bits, and the source of the error packet is not encoded. Moreover, error packets from different nodes can overlap. Therefore, it is difficult to determine which node initiating the error packet when the error occurs. Several studies had been conducted on network reliability under interferences. For example, the work in Ref. [3] uses BER to calculate Poisson error arrival model parameters. However, BER is an averaged error statistics and difficult to measure accurately in practice[25]. The bus-off estimation method in Ref. [5] can only work on polling based networks, and requires logging all the network traffic data. LEI, et al[23], studied model based CAN error monitoring method, however the node MTTB assessment method was not studied. In addition, the framework proposed in Ref. [17] requires major upgrade on the network hardware, which is usually not possible on existing systems. As it can be seen from the literature, the existing methods are difficult to directly apply on the practical CAN systems. Moreover, the two challenges stated above still remain and need to be solved. Therefore, a systematic node MTTB assessment method for CAN-based networks is dearly needed given that it is essential for system health evaluation and monitoring.

The aim of this paper is to develop a novel data driven node time to bus-off assessment method for CAN networks by directly using the network error event data. The main advantages of the proposed method are in three folds: First, only the network errors are recorded and analyzed, which is easy to implement and reduces the complexity of data processing. Second, the MTTB of the node is directly estimated from the collected error information using a stochastic model. This approach describes stochastic behavior of the network errors, which is better than using the models derived from indirect averaged statistical measures. Third, the proposed method in this work is non-intrusive, which collects the error information passively without interrupting the system operation. The result of this work will enable one to have a clear overview of the health status of the network nodes under current interference condition, which should ultimately lead to rapid evaluation and improvements of the system health management.

The rest of the paper is organized as follows: fault confinement mechanism of CAN network is briefly introduced in section 2, followed by formal definition of the problem in section 3. Section 4 implements the methodology of modeling process, followed by experimental setup in section 5. Experiments results are discussed in section 6 and section 7. Finally, conclusion and future work are provided in section 8.

2 Fault Confinement Mechanism of CAN

As defined in CAN specification, a node could be in one of the following three communication states: error active, error passive and bus-off. The state of a node is determined by its embedded TEC value. When the TEC value exceeds 127, this node will switch from error active state to error passive state. If the TEC value reaches threshold (255), this node will turn to bus-off state.

A simplified changing rule of TEC value V_{TEC} is illustrated in Eq. (1), where the increment(ΔV_{TEC}) is determined by the node's communication state as well as its current TEC value.

$$\Delta V_{\mathrm{TEC}}=\begin{cases}0, & \text{frame transmitted, } V_{\mathrm{TEC}}=0,\\ -1, & \text{frame transmitted, } V_{\mathrm{TEC}}\neq 0,\\ 8, & \text{frame transmission failed, } V_{\mathrm{TEC}}\leqslant 255.\end{cases} \tag{1}$$

As a rule of thumb, the TEC value of a node will be increased by 8 when an error is detected during the transmission, except in the following cases: (1) If the node

is in error passive state and detects an acknowledgment error while sending its passive error frame; (2) An error occurred in arbitration fields during transmitting. In these two cases, TEC value would remain unchanged. When a frame is successfully sent, the sending node's TEC value will be decreased by 1, unless it is already 0.

3 Problem Definition

According to CAN fault confinement mechanism, the TEC value of the node is evaluated after a data frame is transmitted. When an error is detected during the transmission, all the nodes will response to this error, and the TEC value of the interrupted node will be increased accordingly. From network health management perspective, it is important to estimate how much time the network can sustain without losing a node under current network interferences. However, in industrial applications, the TEC values of the nodes are generally inaccessible. Therefore, the problem of node MTTB assessment can be defined as

$$T_{\mathrm{MTTB}} = f((E_{\mathrm{t}}),(E_{\mathrm{r}}),T_{\mathrm{P}}), \tag{2}$$

where T_{MTTB} is the MTTB of a node, (E_{t}) denotes the sequence of 6 bits error events, (E_{r}) denotes the sequence of 7–12 bits error events, and T_{P} is the communication cycle of nodes. In other words, given passively acquired network error information including 6 bits error events and 7–12 bits error events, how to estimate the MTTB of the individual node. In this work, we assumed the network communication mode is periodic (e.g. master node controlled polling, remote node controlled periodic transmission, or change-of-state transmission in cyclic operation environments), which are widely used in manufacturing systems.

4 Node Reliability Assessment Method

The overall procedure of the proposed method is illustrated in Fig. 1. As shown in the figure, the proposed node MTTB assessment method consists of three major modules: network error processing module, network error model fitting module and node MTTB prediction module. In network error processing module, the network errors are extracted and analyzed from the recorded multiple-layer network error log. In the network error model fitting module, the extracted network error information is fitted to a generalized zero inflated Poisson process(GZIP) model with an optimized time window, in which the stochastic properties of the network errors are modeled. Finally, in the node MTTB prediction module, the bus-off state prediction model is established by using stochastic information from the network error models. Details of the proposed method are introduced as follows.

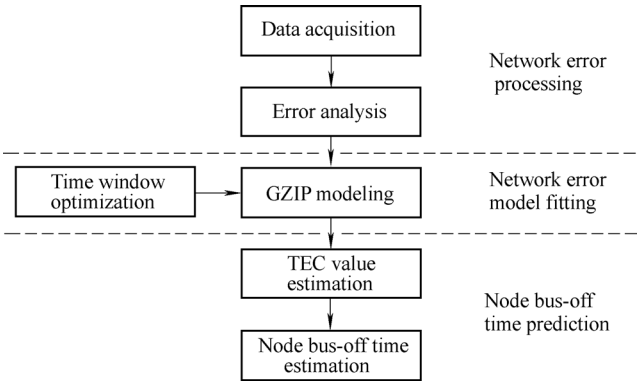

Fig. 1. Overall flowchart of the proposed method

4.1 Network error processing

As mentioned previously, upon each network error, the change of TEC value is determined by the transmission status of the node. Therefore it is important to obtain the transmission status of the nodes upon each error as well as the stochastic properties of the CAN errors. However, the diagnosis information provided by the CAN error frame is very limited due to its simple format. Moreover, in most commercial CAN interface chips, the corrupted data frame will be discarded upon each error. As a result, it is not easy to determine which node's transmission is interrupted. Therefore, a CAN error acquisition and analysis system is developed to retrieve these two important network error information for node MTTB assessment.

The CAN error acquisition and analysis module consists of two functions: (1) error acquisition, (2) error analysis, as shown in Fig. 2.

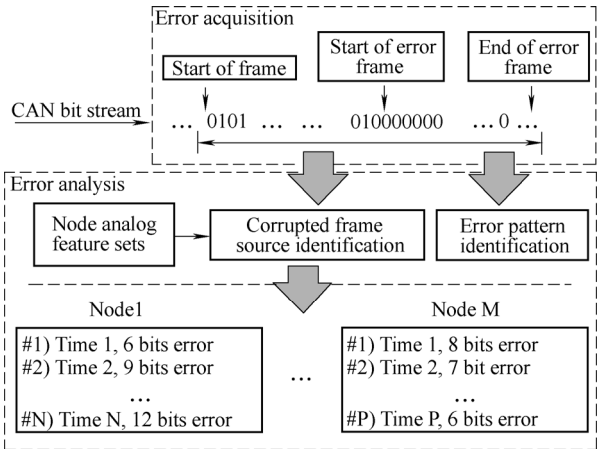

Fig. 2. Structure and functions of the error acquisition and analysis module

In error acquisition function, A Field Programmable Gate Array(FPGA) based multiple-layer error capturer system is developed to record and synchronize all the available error information from data link layer and physical layer. An online error detector circuit is developed to monitor the data link layer bit stream and enable the trigger signal when 6 consecutive dominant bits, a minimal error frame length, are detected. The trigger signal is used to synchronize the data acquisition system which records the physical layer

signal before and after the trigger signal. To detect the end of the error frame, the error detector will continue counting the number of bits after the trigger signal until the error frame ends(by detecting a recessive bit). To detect the beginning of the error frame, physical layer bit signals are used. One needs to analyze the bit analog profile backwards bit by bit from the end of the error frame. As illustrated in Fig. 3, depending on the number of bits (k) after the trigger signal, the beginning of the error frame may vary. If $k=0$, then the bit at point A is the beginning of the error frame. If $k\in[0,6]$, then the first bit that is different from the bit at point C will be the beginning of the error frame, since in this case the error frame is originated from one node and followed by the rest of the nodes.

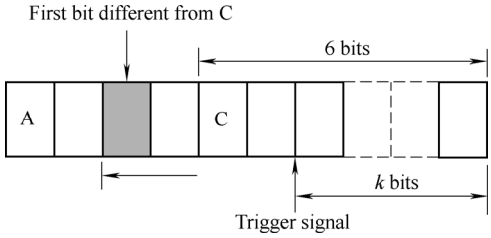

Fig. 3. Detection of the beginning and end of an error frame

In error analysis function, based on the synchronized multiple-layer error log, node addresses of the corrupted transmissions are extracted. If the source addresses in the arbitration fields of the corrupted frames are available, then they can be directly identified. If the source addresses are destroyed, analog feature sets learnt from normal node data frame will be used to extract the source of the corrupted data frame, as suggested in Ref. [26]. In addition, for error modeling purpose, the error patterns are identified based on lengths of the error frames caused by various physical causal factors. The error information extracted from network errors is filtered and rearranged for each node for CAN error modeling. Each error event can be marked as the following quadruple $(t_e, \mathrm{ID}_i, \mathrm{ID}_e, l_e)$, where t_e denotes the error frame occurrence time, ID_i denotes the address of the interrupted node when the error occurs, ID_e denotes the address of the node that originates the error frame(in case of 6 bits error frame, ID_e is omitted), and l_e denotes the total length of the error frame. Hence all the error events that related to a node, either the node address appears in ID_e or ID_i, will be filtered and form a separate event sequence for this node, which will be used for further analysis.

4.2 Network error model fitting

The purpose of CAN error modeling is to describe the stochastic properties of the network errors for node MTTB assessment. Although the reactions of the network nodes follow the same rule upon each error, different error causal factors will result in different types of error frames in terms of error length depending on the affected region and timing. Among these factors, global causal factors usually include system electromagnetic interferences(EMI), grounding problems. Local causal factors usually include intermittent connection problems on the network, node electronic problems, and EMI on single nodes. Therefore an appropriate model needs to be selected to represent the stochastic properties of the errors.

To illustrate the concept of different error types from different causal factors, let us consider intermittent connection induced errors. Consider a CAN network consists of three nodes: a master node(PLC), slave node 8 and node 9, and assume that the intermittent connection problem exists either on the drop cable to node 8(case A) or on the backbone of the network(case B). In case A, if an intermittent connection problem occurs while node 8 is receiving data frame from PLC, only node 8 will detect the error in the received data since other nodes do not receive any error. Hence the error frame is originated by node 8, then node 9 and PLC will response to this error frame shortly. Therefore the total length of the final error frame will be 7–12 bits. On the contrary, if an intermittent connection occurs while node 8 is transmitting a data frame, node 9 and PLC will response to the error and send error frames simultaneously. Thus, the error frame will be 6 bits. As a result, localized intermittent connection problem will generate two types of error frames: 6 bits error frames and 7–12 bits error frames. In case B, on the contrary, the network is divided into two groups by the intermittent connection point on the backbone. Therefore at any time, only one group will include the node that is transmitting data, and the node within this group will not notice any error when intermittent connection problem occurs, while the node in the other group will send the error frames firstly. Therefore it will only generate 7–12 bits error frames.

As discussed above, there are two kinds of errors are related to each node, which are 6 bits error and 7–12 bits error. In this case, it is inappropriate to use a Poisson distribution to model all the errors related to each node. In this section, in order to model two different kinds of errors, the generalized zero inflated Poisson process model is adapted by imposing time windows on time stamped error data[24, 27]. A GZIP model for CAN network errors can be expressed as follows:

$$\begin{cases} P(X=0)=1-\sum\limits_{i=1}^{n}\lambda_i+\sum\limits_{i=1}^{n}\lambda_i\exp(-\mu_i), \\ P(X=x)=\sum\limits_{i=1}^{n}\lambda_i\dfrac{\mu_i^x\exp(-\mu_i)}{x!}, \end{cases} \tag{3}$$

where X denotes the number of errors within a time window, λ_i and μ_i represents the rate of the i-th shock and the average level parameter of each distribution respectively. In this paper, considering 6 bits and 7–12 bits errors, we would have $n=2$, and $\theta=(\lambda_t,\mu_t;\lambda_r,\mu_r)$ are the corresponding GZIP model parameters, where λ_t and μ_t indicates the occurrence probability and the mean value of

the 6 bits error, λ_r and μ_r indicates the occurrence probability and the mean value of the 7–12 bits error, respectively.

Given a sequence of error counting in N time windows $E_N=[X_1,X_2,\cdots,X_N]$, where X_i denotes the total number of errors within i-th window, θ can be estimated by

$$\begin{cases}\lambda_i^{k+1}=\dfrac{1}{N}\displaystyle\sum_{q=1}^{N}\Pr(i\mid X_q,\theta^k),\\ \mu_i^{k+1}=\dfrac{\displaystyle\sum_{q=1}^{N}X_q\bullet\Pr(i\mid X_q,\theta^k)}{\displaystyle\sum_{q=1}^{N}\Pr(i\mid X_q,\theta^k)},\end{cases}\quad i\in\{t,r\},\tag{4}$$

where $Pr(i\mid X_q,\theta^k)$ denotes the posterior probability that X_q comes from the i-th error event given the presently iterated parameters θ^k, which is calculated as

$$\Pr(i\mid X_q,\theta^k)=\frac{\lambda_i^k P_i(X_q\mid\mu_i^k)}{\displaystyle\sum_{j=0}^{N}\lambda_j^k P_j(X_q\mid\mu_j^k)}.\tag{5}$$

In this paper, the initial values setting rule is proposed as

$$\begin{cases}\lambda_i^0=(1-\lambda_0)N_i/N_{\text{tol}},\\ \mu_i^0=N_i\bullet T_w/t_{\max},\end{cases}\quad i\in\{t,r\},\tag{6}$$

where λ_0 denotes the ratio of zeros in E_N, T_{w} denotes the duration of the time window, $t_{\max}$ is the recording time, and N_i, N_{tol} stands for the numbers of i-th type of error and sum total of observations in the data log, respectively.

Moreover, the likelihood confidence domain is used to obtain the confidence interval of GZIP model parameters. Let us assume the following hypothesis: $H_0:\theta=\hat{\theta}$, $H_1:\theta\neq\hat{\theta}$, and the rejection region W can be described as

$$W=\{x\mid 2\ln\lambda(x)>\chi^2_{1-\alpha}(k)\},\tag{7}$$

$$\lambda(x)=\frac{\displaystyle\prod_{i=1}^{n}p(X_i;\hat{\theta})}{\displaystyle\prod_{i=1}^{n}p(X_i;\theta_0)},\tag{8}$$

where $\hat{\theta}$, θ_0 denotes the estimated and true value of modeling parameters, respectively. From Eq. (7) and Eq. (8), it can be inferred as

$$\{\Theta:2\ln\lambda(x;\theta)\leqslant\chi^2_{1-\alpha}(k)\}=\{\Theta:2\ln\left\{\frac{\displaystyle\prod_{i=1}^{n}p(X_i;\hat{\theta})}{\displaystyle\prod_{i=1}^{n}p(X_i;\theta_0)}\right\}\leqslant\chi^2_{1-\alpha}(k)\},\tag{9}$$

where Θ is the confidence interval with confidence level $1-\alpha$, and k represents the dimension of parameters.

In addition, the optimal time window(T_{opw}) is a significant factor in the GZIP model, since if the value of time observation window is too large, it filters the diversity of probability, otherwise there exists little difference between frequency of error frames with a small window. T_{opw} is determined by minimizing the differences between the model and data in terms of probability density function:

$$T_{\text{opw}}=\min_{T_{\text{w}}}\left\{\sum_{k=0}^{\infty}|f^i_{\text{model}}(k)-f_{\text{data}}(k)|\right\},\tag{10}$$

where $f^i_{\text{model}}(k)$ denotes the probability density function of the model after i-th iteration, $f_{\text{data}}(k)$ denotes the normalized histogram of the data, and k denotes the error index.

4.3 Node mean time to bus-off prediction

In previous subsection, for each node, we assumed the errors related to this node follow a GZIP distribution (related means this node is transmitting a data frame when an error occurs). Moreover, as shown in Eq. (1), the increment of this node's TEC value is a stochastic process, that is, consider $\{Y_n,n\leqslant 1\}$ as a sequence of independent random variable, where Y_n denotes the increment of the TEC on n-th failed transmission of this node. Let T_n denote the minimum number of errors needed for this node going to bus-off state, that is, its TEC value reaches 256. Therefore, we had

$$T_n=\min\left\{n:\sum_{i=1}^{n}Y_i=256\right\}.\tag{11}$$

Since T_n is a stopping time for Y_n, according Wald's equation, the following equation holds

$$\mathrm{E}\left[\sum_{n=1}^{T_n}Y_n\right]=(\mathrm{E}[Y])(\mathrm{E}[T_n]),\tag{12}$$

where $\mathrm{E}[T_n]$ denotes the expectation of T_n.

Then, the expected time to reach bus-off state can be calculated by Eq. (11) and Eq. (12), as shown in Eq. (13):

$$T_{\text{bus-off}}=T_n\bullet\frac{T_{\text{opw}}}{\mathrm{E}[N]}=\frac{256}{\mathrm{E}[Y]}\bullet\frac{T_{\text{opw}}}{\mathrm{E}[N]},\tag{13}$$

where $\mathrm{E}[N]$ denotes the expected number of transmission errors within T_{opw}.

Given a sequence of time stamped errors related to a node, one can fit a GZIP distribution model with the optimized time window, and use the probability density function expressed in Eq. (3) to calculate $\mathrm{E}[Y]$. Let us assume there are f_k number of observation windows with

k errors (k=0,1,⋯) in the data log obtained from previous subsection, the increments of TEC in such a time observation window can be determined by

$$\Delta V_{\mathrm{TEC}_k} = P(X=k)\cdot\left(8\cdot k\cdot f_k - \frac{1}{1+\mathrm{E}[N]}\cdot\frac{T_{\mathrm{opw}}}{T_p}\right), \quad (14)$$

where $\left(\frac{1}{1+\mathrm{E}[N]}\cdot T_{\mathrm{opw}}/T_p\right)$ represents the expected number of successful transmission in a time window, and T_p denotes the communication cycle of this node, $P(X=k)$ is the probability density of the fitted GZIP distribution in Eq. (3).

Therefore, for all possible k errors within timing windows, we had

$$\mathrm{E}[Y] = I\cdot\sum_{k=1}^{m}\Delta V_{\mathrm{TEC}_k} + \sum_{k=m+1}^{n}\Delta V_{\mathrm{TEC}_k} \quad (15)$$

where I is an indicator ($I=1$ only if $\sum_{k=1}^{m}\Delta V_{\mathrm{TEC}_k}\geqslant 0$, otherwise $I=0$), and n is determined by the maximum number of errors measured within each timing window. The indicator I is introduced to ensure that $V_{\mathrm{TEC}}\geqslant 0$.

5 Test Bed Setup

To demonstrate the proposed method, a laboratory DeviceNet based test-bed has been constructed, which uses CAN protocol in its physical layer and data link layer. The schematic layout of the test bed is shown in Fig. 4. The test-bed consists of a master device(PLC) and several remote I/O nodes. The network sets a polling mode with communication speed at 500 kbps. The test bed also includes the in-house developed network data logging system and a network error injection system, as shown in Fig. 5. Additionally, a network error frame capturer is developed to trigger the network error frame acquisition using the network data logging system, in which the length and time stamp of each error frame can be analyzed in real time.

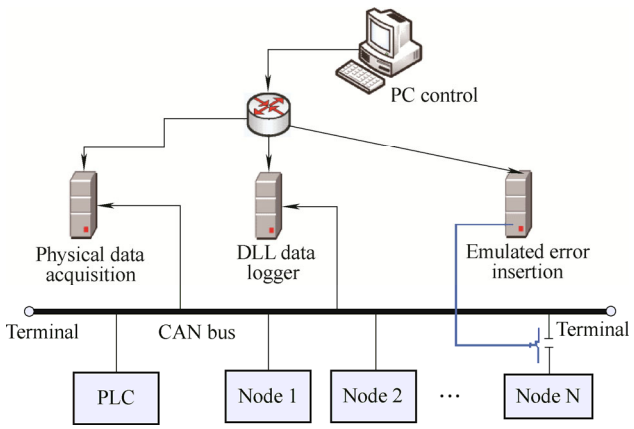

Fig. 4. Schematic layout of the test bed

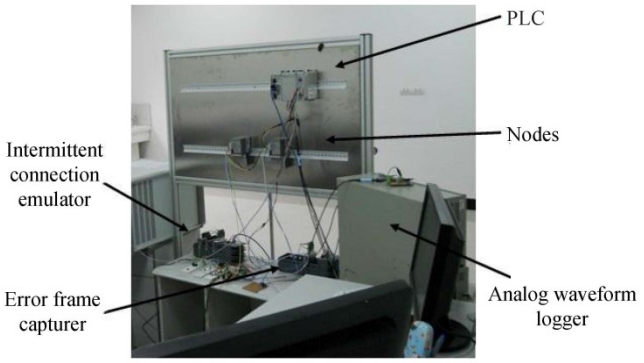

Fig. 5. Test bed system for network MTTB assessment

The network errors are injected by emulating the intermittent open-circuit connection problems, one of the major failure modes in industrial applications, using a computer controlled high-speed analog switch on a drop cable. There are two reasons of using the intermittent connection problem on the drop cable of the network in the case studies: First, it will create both 6 bits and 7–12 bits error frames. The patterns of two types of frames are consistent when multiple faults exist simultaneously. Second, not only the node that has the intermittent connection problem can be offline, sometimes the nodes without the problems can be offline as well, which is very special among other causal factors. The interval between two open-circuit events of the switch follows a Poisson distribution, as shown in Eq. (16):

$$P(\delta T=k) = \frac{\exp(-\mu)\mu^k}{k!}, \quad (16)$$

where μ denotes the mean interval time of the Poisson distribution, which controls the emulated error injection rate, k denotes the random time interval between two consecutive error events. Please note that although the open-circuit events follow a Poisson distribution, the resultant errors do not follow a Poisson distribution since the open-circuit event during network idle period will not trigger an error.

6 Case Studies

In this section, the proposed method is demonstrated through accelerated case studies with different error injection rates. The brief descriptions of case studies are shown in Table 1. The average error injection intervals shown in Table 1 are the carefully chosen so that the node can switch into bus-off state in a reasonable shorter span of time.

In the first case study, we illustrated the analysis procedures for the nodes in detail. In the second case study, different error injection rates were used to demonstrate the effects of errors on the MTTB of the nodes. In the third case study, we demonstrated that the node without connection problems can go offline. In the last case study,

we demonstrated that the proposed method works well on multiple faults scenario. In the first three case studies, the network consists of three nodes, specifically, PLC, node 8 and node 9. Moreover, the intermittent connections are emulated on the drop cables of node 8. In the last case study, there are 5 nodes on the bus, which are PLC, node 5, node 7, node 8 and node 9. In order to represent the multiple faults scenario, the intermittent connections are emulated on the drop cables of node 5 and node 9, respectively.

Table 1. Settings and purposes for different case studies

Case studies	Network topology	Average error injection interval t/ms	Purpose
1	3-node network	1.1	Illustrate the analysis procedures
2	3-node network	1	MTTB prediction with different error injection rate
3	3-node network	1	Special phenomenon
4	5-node network	1.4 for node 5 2.2 for node 9	Multiple faults scenario

6.1 Case study 1

In this case study, we demonstrated the procedures of the MTTB assessment for two nodes. The first one is node 8 which has intermittent connection problems, and the second one is node 9 which is free of intermittent connection problems. We set the average error injection interval time μ in Eq. (16) as 1.1 ms. First, we demonstrated the analysis procedures for node 8. From the recorded error information, $T_{\text{opw}} = 0.772$ s can be obtained by Eq. (10), which is used to establish the error events distribution GZIP model of node 8. Fig. 6 shows the comparison of the fitted GZIP model with the histogram of the number of errors within the optimal time window. Based on the Eqs. (4)–(9), the GZIP model parameters $\theta(\lambda_t, \mu_t; \lambda_r, \mu_r)$ as well as their confidence intervals can be determined, as shown in Table 2.

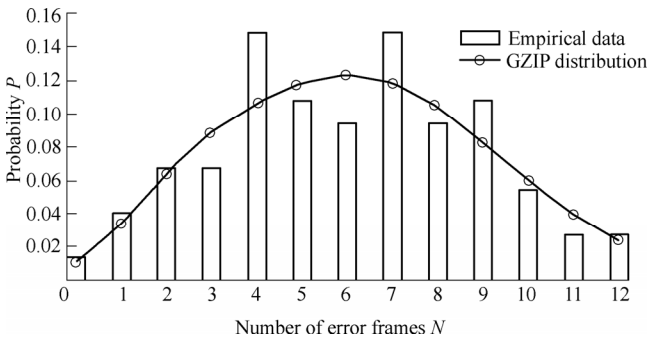

Fig. 6. Distribution of the number of errors of node 8 within its optimal time window in case study 1

Table 2 shows the estimated TEC value as well as the MTTB of node 8. As shown in the table, the estimated TEC value of node 8 almost reaches the threshold 256. The predicted bus-off time agrees well with the observed value (55.8 s), and the observed bus-off time is within the estimated range of the $T_{\text{Bus-off}}$.

Table 2. Parameters of node 8 which reaches bus-off state at 55.8 s in case study 1 (T_{opw}=0.772 s)

Parameters	Point estimation	Upper limit	Lower limit
λ_t	0.255 4	0.255 4	0.094 6
μ_t	3.340 9	3.343 8	0.246
λ_r	0.743	0.743	0.519 2
μ_r	7.285 5	9.000 2	7.283
$E(TEC)$	255.2	255.36	253.24
$T_{\text{Bus-off}}$ t/s	57.31	95.72	55.38

Table 3 illustrates the estimation results using different time windows T_{w}. The table shows positive correlation between the estimated value and the time window, because larger time window will include higher percentage of successful transmissions, which results in lower TEC value and longer bus-off time. As it can be seen from the table, the result using the optimal time window ($T_{\text{opw}} = 0.772$ s) is much more consistent with the actual value.

Table 3. Bus-off times in different time window T_{w} in case study 1 (node reaches bus-off at 55.8 s)

T_{w} t/s	$T_{\text{Bus-off}}$ t/s	Upper limit t/s	Lower limit t/s
0.772	57.31	95.72	55.38
0.556	42.30	64.00	28.90
0.704	51.17	73.13	38.30
1.041	81.20	148.27	49.692 1

Secondly, we demonstrated the analysis results for node 9. Similar to the analyzing procedures for node 8, by fitting the error GZIP model with the optimized time window ($T_{\text{opw}} = 0.677$ s), the model parameters $(\lambda_t, \mu_t; \lambda_r, \mu_r) = (0.321\,9, 1.514\,2; 0.669\,7, 4.593\,6)$ for node 9 can be determined. The estimated TEC value and the estimated MTTB of node 9 are shown in Table 4.

Table 4. Parameters of node 9 without reaching bus-off in case study 1

$T_{\text{opw}} = 0.677$ s	$E(TEC)$	$T_{\text{Bus-off}}$ t/s
Point estimation	181.07	77.53
Upper limit	182.87	199.88
Lower limit	179.75	65.64

Fig. 7 shows the comparison of the distribution of the fitted GZIP model with the histogram of the data. As shown in Fig. 7, the GZIP model of node 9 shows different stochastic properties from node 8, because node 9 does not have intermittent connection problem, and the governing natures of the error generation of two nodes are completely different, specifically, the probability of successful transmitting of the node 8 is lower than node 9. Moreover, the expected number of errors within the time window of

node 8 is larger than that of node 9, because node 8 is affected directly by the intermittent connection problem. In addition, further analysis shows that node 9 is in the error passive state when node 8 reaches bus-off state, which indicates that the estimated TEC value using our proposed method is within a reasonable range. Furthermore, by comparing to node 8, it is noted that the estimated MTTB of node 9 is significantly longer than that of node 8, which is expected since the node with intermittent connection problem has the tendency to fail first.

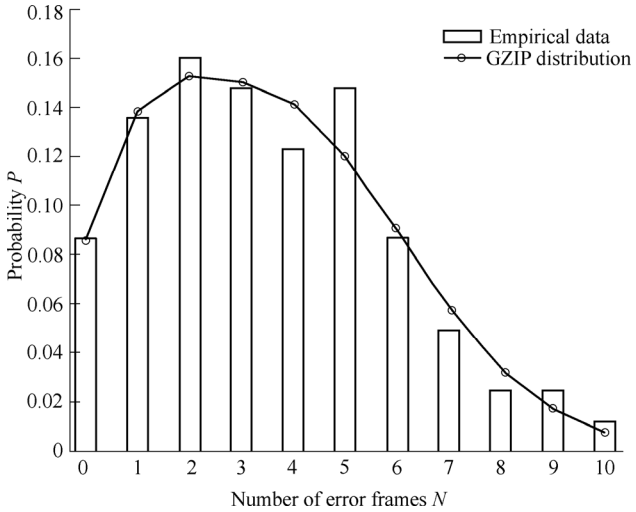

Fig. 7. Distribution of the number of errors related to node 9 within time window in case study 1

In addition, the comparison between GZIP model with single event stochastic models like Poisson or geometric models are shown in Fig. 8, which uses the error data from node 9. The comparison result shows that GZIP model is preferred, which is expected because there are two kinds of errors are related to each node and the GZIP model can represent the events with different labels, while the Poisson model and Geometric model can only represent one kind of event.

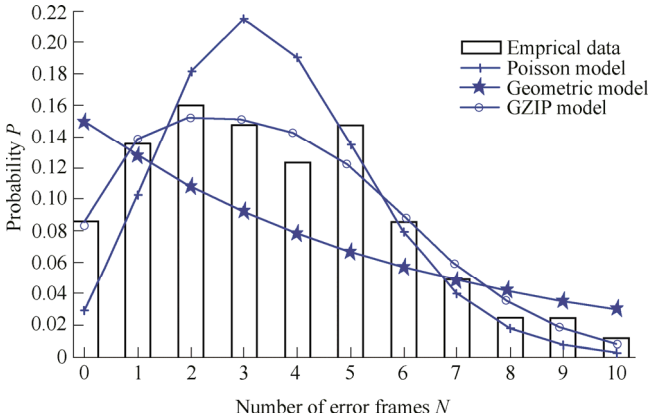

Fig. 8. Comparison of the probability density functions of different models using the error event data from node 9

6.2 Case study 2

In this case study, we illustrated the impacts of higher error rates on the node MTTB assessments. The degradation of the network connection problems is realized by reducing the average error injection interval from 1.1ms to 1ms. Comparing to case study 1 in which node 8 turns to bus-off state at 55.8 s, in this case study, the observed bus-off time of node 8 is 43 s. The errors occur in higher frequency, and hence the bus-off phenomenon occurs faster. The estimated model parameters of node 8 are shown in Table 5.

Table 5. Parameters of node 8 which reaches bus-off state at 43 s in case study 2 (T_{opw}=0.524 s)

Parameters	Point estimation	Upper limit	Lower limit
λ_t	0.634 7	0.641	0.628 8
μ_t	3.880 5	8.340 2	3.878 3
λ_r	0.285 1	0.289 7	0.276 8
μ_r	3.796 1	10.919 9	3.793 1
$E(TEC)$	251.25	252.66	250.16
$T_{\text{Bus-off}}$ t/s	44.31	72.49	29.08

As expected, higher error injection rate contributes to lower successful transmission rate, which weakens the accuracy of TEC estimation. That is, lower error injection rate contributes to more accurate prediction of the node MTTB, since the GZIP model requires higher rate of successful transmission by definition. Nevertheless, as shown in Table 5, even in the extreme harsh setup of the test bed, the predicted bus-off time agrees with the actual bus-off time ($T_{\text{Bus-off}}$) of nodes.

Similar to the procedure demonstrated in case study 1, we could estimate the MTTB of node 9, which is

$$T_{\text{Bus-off}} = 60.36\ s \subseteq [46.09\ \text{s}, 279.87\ \text{s}], \tag{17}$$

It is noted that the MTTB of the node 9 is significantly longer than node 8, since node 8 is affected directly by the intermittent connection problems.

6.3 Case study 3

In this case study, we demonstrated a special phenomenon that may occur in practice where the node without intermittent connection problem can be affected by remote problematic node, and turn to bus-off state before the problematic node does. The average error injection time interval in this experiment is set to 1 ms. Based on the proposed methods, the model parameters as well as the MTTB of the nodes are shown in Table 6, where node 9 turns to bus-off state at 89.4 s.

Table 6. Model parameters and estimated MTTB of the nodes in case study 3

Parameters	Node 9	Node 8
T_{opw} t/s	1.257	0.968
λ_t	0.039 5	0.492 5
μ_t	1.997 8	6.830 3
λ_r	0.955 4	0.499 6
μ_r	7.133	8.709
$T_{\text{Bus-off}}$ t/s	92.79 ⊂ [71.64,96.72]	94.86 ⊂ [75.44,140.49]

Comparing with case study 2 where the problematic node, i.e., node 8 turned to bus-off firstly, in this particular case, the predicted TEC value of node 9 almost reaches the threshold, and the node 9 turns to bus-off first at 89.4 s. As shown in Table 6, our method can effectively tackle this special phenomenon, the actual bus-off time of node 9 is within the confidence interval of the $T_{\text{Bus-off}}$, and the predicted MTTB of node 9 agrees well with the actual value.

6.4 Case study 4

In this study, we demonstrated that the proposed method works well on multiple faults scenario. As mentioned earlier, the intermittent connections are emulated on the drop cables of node 5 and node 9, respectively. The average error injection intervals are 1.4 ms for node 5 and 2.2 ms for node 9, respectively. The result shows that node 5 reaches the bus-off state firstly at 20.16 s. Using the proposed analyzing procedures, the estimated TEC value and bus-off time are shown in Table 7. As it can be seen, the predicted bus-off time agrees well with the observed value, and the actual bus-off time is within the confidence interval of the $T_{\text{Bus-off}}$.

Table 7. Parameters of node 5 which reaches bus-off state at 20.16 s in case study 4 (T_{opw}=0.198 s)

Parameters	Point estimation	Upper limit	Lower limit
λ_t	0.954 5	0.958 9	0.948 6
μ_t	1.810 4	3.632 1	1.809 4
λ_r	0.037 5	0.041 0	0
μ_r	1.422 4	7.541 8	1.388 1
$E(TEC)$	244.30	245.03	243.98
$T_{\text{Bus-off}}$ t/s	20.54	27.41	12.57

7 Discussion

In this paper, according to Eq. (13), the estimation accuracy of the node MTTB is determined by the estimated GZIP model, which is not directly related to the communication speed of the network. In practice, for monitoring or diagnosis purposes, the network is usually given, and the communication speed cannot be changed in production systems. However, given the same network communication setup, faster communication speed will result in shorter transmission time and longer network idling time. Therefore, given the same error condition, the rate of successful transmission will be higher, which has similar effects as lower error occurrence rate under the same network speed. In this paper, by comparing case study 1 and 2, we could see that lower error occurrence rate will slightly increase the accuracy of the estimation, but the improvement is not significant.

In addition, the methodology proposed in this paper is general and can be applied to scenarios with multiple faulty nodes or fault modes, since these two scenarios will also generate aforementioned 6 bits and/or 7–12 bits error frames. In either scenarios, appropriate GZIP model order should be selected. Since the GZIP model can represent the mixture of different Poisson models, ideally if the number of faulty nodes or fault modes(k) is known, we could determine the order of the model accordingly as $n = k \times 2$ in Eq. (3). However, in practice k is usually unknown, therefore we could take a numerical approach: let us initially set the order of the GZIP model according to the number of error types ($n = 2$, that is $k = 1$), then increase the model order gradually ($k = 2, \cdots$). Since the tradeoff between model complexity and accuracy is needed to take, hence if the difference between the probability density function of the fitted model and the data does not decrease significantly (*5%*), then the appropriate model can be selected.

8 Conclusions

(1) A new data driven node mean time to bus-off assessment method for CAN network is developed by directly using network error information.

(2) A GZIP model is constructed to describe the distribution of the error frames in each observation timing window.

(3) Accelerated experiments are conducted on a laboratory CAN network and the network errors are generated by a computer controlled error injection system. The experimental results demonstrated in this paper agree well with the observations, which show the accuracy and effectiveness of the proposed method.

Future work includes improving current method by integrating TEC value observations from one or more TEC-accessible nodes, and developing robust node MTTB assessment method using incomplete network information.

References

[1] YANG Z, KAN Y, CHEN F, et al. Bayesian reliability modeling and assessment solution for NC machine tools under small-sample data[J]. *Chinese Journal of Mechanical Engineering,* 2015, 28(6): 1229–1239.

[2] WANG Y, ZHANG F, CUI T, et al. Fault diagnosis for manifold absolute pressure sensor(MAP) of diesel engine based on Elman neural network observer[J]. *Chinese Journal of Mechanical Engineering,* 2016, 29(2): 386–395.

[3] GAUJAL B, NAVET N. Fault confinement mechanisms on CAN: analysis and improvements[J]. *IEEE Transactions on Vehicular Technology,* 2005, 54(3): 1103–1113.

[4] CHEN J, LUO F, SUN Z. Reliability analysis of CAN nodes under electromagnetic interference[C]*//IEEE International Conference on Vehicular Electronics and Safety,* Beijing, China, Dec 13–15, 2006: 367–371.

[5] LEI Y, DJURDJANOVIC D, NI J. DeviceNet reliability assessment using physical and data link layer parameters[J]. *Quality and Reliability Engineering International,* 2010, 26(7): 703–715.

[6] CAUFFRIEZ L, CONRARD B, THIRIET J M, et al. Fieldbuses and their influence on dependability[C]*//IEEE IMTC 2003 Instrumentation and Measurement Technology Conference.* VAIL, CO, United States, May 20–22, 2003, 2: 1005–1008.

[7] JUMEL F, THIRIET J M, AUBRY J F, et al. Toward an Information-Based Approach for the Dependability Evaluation of Distributed Control Systems[C]*//IEEE Instrumentation and*

Measurement Technology Conference, VAIL, CO, United States, May 20–22, 2003, 1: 270–275.

[8] CORNO F, PEREZ J, RAMASSO M, et al. Validation of the dependability of CAN-based networked systems[C]*// Proceedings of the Ninth IEEE International High-Level Design Validation and Test Workshop,* Sonoma Valley, CA, USA, Nov 10–12, 2004: 161–164.

[9] HANSSON H A, NOLTE T, NORSTRÖM C, et al. Integrating reliability and timing analysis of CAN-based systems[J]. *IEEE Transactions on Industrial Electronics,* 2002, 49(6): 1240–1250.

[10] GUJARATI A, AGGARWAL A, CLEMENT A, et al. Probably Right, Probably on Time: An Analysis of CAN in the Presence of Host and Network Faults [C]*// 21st IEEE Real-Time and Embedded Technology and Applications Symposium,* Seattle, USA, April 13–17, 2015: 9–10.

[11] TRAN E, KOOPMAN P. *Multi-bit error vulnerabilities in the controller area network protocol*[M]. Pittsburgh: Carnegie Mellon University Press, 1999.

[12] RODRÍGUEZ-NAVAS G, JIMENEZ J, PROENZA J. An architecture for physical injection of complex fault scenarios in CAN networks[C]*//IEEE Conference on Emerging Technologies and Factory Automation,* Lisbon, Portugal, Sep 16–19, 2003, 2: 125–128.

[13] REORDA M S, VIOLANTE M. On-line analysis and perturbation of CAN networks[C]*//19th IEEE International Symposium on Defect and Fault Tolerance in VLSI Systems,* Cannes, France, Oct 10–13, 2004: 424–432.

[14] SHORT M, SHEIKH I, ALEY S, et al. Bandwidth-efficient burst error tolerance in TDMA-based CAN networks[C]*//IEEE 16th Conference on Emerging Technologies & Factory Automation,* Toulouse, France, Sep 5–9, 2011: 1–8.

[15] CHEN H, TIAN J. Research on the controller area network[C]*//IEEE International Conference on Networking and Digital Society,* Guiyang, China, May 30–31, 2009, 2: 251–254.

[16] CENA G, BERTOLOTTI I C, HU T, et al. Software-based assessment of the synchronization and error handling behavior of a real CAN controller[C]*//IEEE 18th Conference on Emerging Technologies & Factory Automation,* Cagliari, Italy, Sep 10–13, 2013: 1–9.

[17] BARRANCO M, PROENZA J, RODRÍGUEZ-NAVAS G, et al. An active star topology for improving fault confinement in CAN networks[J]. *IEEE Transactions on Industrial Informatics,* 2006, 2(2): 78–85.

[18] YARAMASU A, CAO Y, LIU G, et al. Intermittent wiring fault detection and diagnosis for SSPC based aircraft power distribution system[C]*//IEEE/ASME International Conference on Advanced Intelligent Mechatronics,* Kaohsiung, Taiwan, China, Jul 11–14, 2012: 1117–1122.

[19] BARRANCO M, PROENZA J. Towards understanding the sensitivity of the reliability achievable by simplex and replicated star topologies in CAN[C]*//IEEE 16th Conference on Emerging Technologies & Factory Automation,* Toulouse, France, Sep 5–9, 2011: 1–4.

[20] BARRANCO M, PROENZA J, ALMEIDA L. Quantitative comparison of the error-containment capabilities of a bus and a star topology in CAN networks[J]. *IEEE Transactions on Industrial Electronics,* 2011, 58(3): 802–813.

[21] PRODANOV W, VALLE M, BUZAS R. A controller area network bus transceiver behavioral model for network design and simulation[J]. *IEEE Transactions on Industrial Electronics,* 2009, 56(9): 3762–3771.

[22] ZHAO J, LEI Y. Modeling for early fault detection of intermittent connections on controller area networks[C]*//IEEE/ASME International Conference on Advanced Intelligent Mechatronics,* Kaohsiung, Taiwan, China, Jul 11–14, 2012: 1135–1140.

[23] LEI Y, YUAN Y, ZHAO J. Model-based detection and monitoring of the intermittent connections for CAN networks[J]. *IEEE Transactions on Industrial Electronics,* 2014, 61(6): 2912–2921.

[24] LEI Y, YUAN Y, SUN Y. Fault location identification for localized intermittent connection problems on CAN networks[J]. *Chinese Journal of Mechanical Engineering,* 2014, 27(5): 1038–1046.

[25] FERREIRA J, OLIVEIRA A, FONSECA P, et al. An experiment to assess bit error rate in CAN[C]*//Proceedings of 3rd International Workshop of Real-Time Networks (RTN2004),* Catania, Italy, Jun 29, 2004: 15–18.

[26] LEI Y, DJURDJANOVIC D. Diagnosis of intermittent connections for DeviceNet[J]. *Chinese Journal of Mechanical Engineering,* 2010, 23(5): 606–612.

[27] CHEN N, ZHOU S, CHANG T S, et al. Attribute control charts using generalized zero-inflated Poisson distribution[J]. *Quality and Reliability Engineering International,* 2008, 24(7): 793–806.

Biographical notes

ZHANG Leiming, is currently a PhD candidate at *State Key Laboratory of Fluid Power & Mechatronic Systems, Zhejiang University, China.* He received his BS degree in mechanical engineering from *Harbin Institute of Technology, China.*
E-mail: lmzhang@zju.edu.cn

YUAN Yong, received his MS degree in mechanical engineering from *Zhejiang University, China.*
E-mail: 21125110@zju.edu.cn

LEI Yong, born in 1976, is an associate professor at *State Key Laboratory of Fluid Power & Mechatronic Systems, Zhejiang University, China.* He received his BS degree in control science and engineering from *Huazhong University of Science and Technology, China,* his MS degree in manufacturing and automation from *Tsinghua University, China,* and his PhD degree in mechanical engineering from *University of Michigan, Ann Arbor, USA*. His research interests include monitoring and fault diagnosis of the networked automation systems, statistical quality control, and surgical robots.
E-mail: ylei@zju.edu.cn